A NOVEL TENSOR-BASED FEATURE EXTRACTION METHOD FOR POLSAR IMAGE CLASSIFICATION

Xiayuan Huang[1], *Xiangli Nie*[1], *Hong Qiao*[1], *Bo Zhang*[2]

[1]State Key Lab of Management and Control for Complex Systems, Institute of Automation, Chinese Academy of Sciences, Beijing 100190, China,
[2]State Key Lab of Scientific and Engineering Computing and Institute of Applied Mathematics, AMSS, Chinese Academy of Sciences, Beijing 100190, China

ABSTRACT

Spatial information helps improve the performance of polarimetric synthetic aperture radar (PolSAR) image classification. Some existing methods have combined the spatial information and polarimetric features by the third-order tensor representation for feature extraction. They describe a pixel with the patch centered on this pixel. But they neglect the spatial heterogeneity, which may influence the classification performance. Therefore, we firstly seek k nearest samples based on the polarimetric feature similarity for each pixel to construct the second-order tensor, whose first order denotes the nearest samples and the second order denotes the polarimetric features. Moreover, k nearest samples are searched in a spatial local region rather than the full image, which can exploit the spatial information and reduce the computational burden. Then we employ tensor principal component analysis (TPCA) to extract low-dimensional features. Experimental results demonstrate that the proposed method can improve the classification performance compared with other methods.

Index Terms— spatial heterogeneity, tensor-based dimensionality reduction, PolSAR image classification, feature extraction

1. INTRODUCTION

Polarimetric synthetic aperture radar (PolSAR) can acquire rich information of different types of land cover based on multiple polarizations, thus PolSAR image classification has become a research hotspot [1]. General PolAR image classification methods contain two key steps: feature extraction and classifier design. Feature extraction is a crucial factor for PolSAR image classification. Whether the extracted features are proper influences the classification performance to a large extent.

Originally, researchers obtained features from the PolSAR data for image classification [2]. Afterwards, with the advent of various polarimetric target decomposition methods, numerous parameters produced by these target decomposition methods have been utilized as features for image classification [2]. In some recent works, some visual features, such as texture features and color features have also been applied in PolSAR image classification [2]. It is obvious that these features are redundant and their number is huge.

To extract proper low-dimensional intrinsic features, some dimensionality reduction methods have been used for PolSAR image classification, such as Laplacian eigenmaps (LE) [3] and supervised graph embedding (SGE) [4]. However, the above dimensionality reduction methods are based on vectors and deal with a single pixel. In fact, the spatial information is helpful for improving the classification performance. In [1, 5, 6], each pixel was described by the patch centered on this pixel to utilize the spatial information, thus each pixel was represented as a third-order tensor which combined the spatial information and multiple features. Some tensor-based dimensionality methods were used to extract low-dimensional features, such as tensor principal component analysis (TPCA) [5], tensor local discriminant analysis (TLDE) [6], tensor locally linear embedding (TLLE) [1]. These methods indeed take the spatial information into account, but they ignore the spatial heterogeneity. When the patch contains many pixels whose properties are different from the center pixel, it may not be a good choice any more to directly use the patch to characterize the center pixel which has been discussed in [6].

Motivated by the above works, we aim to propose a novel tensor-based feature extraction method which takes the spatial heterogeneity into account in this paper. Firstly, we search k nearest samples of each pixel in a spatial local region based on the polarimetric feature similarity. Then each pixel is represented as a second-order tensor, whose first order denotes the nearest samples and the second order denotes the polarimetric features. Afterwards, we take a simple tensor-based dimensionality reduction method, TPCA, as an example to extract low-dimensional features for PolSAR image classification. Experimental results show that the proposed method can improve the classification performance.

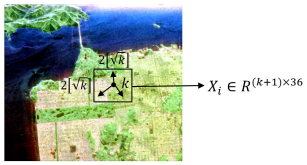

Fig. 1. The process of forming the second-order tensor.

2. THE PROPOSED METHOD

2.1. Polarimetric features

For each pixel, we acquire 36 polarimetric features from the PolSAR data (the scattering matrix S, the coherency matrix T and the covariance matrix C) and some target decomposition methods (Pauli decomposition, H/A/α decomposition, Huynen decomposition, Freeman decomposition and Krogager decomposition). We denote polarimetric features of pixel i by a vector $x_i \in R^{36}$.

2.2. Forming two-order tensors

To consider the spatial heterogeneity, we do not directly adopt the patch to characterize the center pixel. We firstly search k nearest samples of a pixel based on the Euclidean distance of polarimetric features in a local region as described in Fig. 1. The Wishart distance is commonly used as the similarity for PolSAR image classification, but it costs much computation time [7]. While polarimetric features from the PolSAR data and target decomposition methods can also character the property of each pixel. And the computation of he Euclidean distance of polarimetric features is more efficient. Therefore, the Euclidean distance of polarimetric features is used as the similarity in this paper. In addition, the search is conducted in a spatial local region rather the full image, which has two advantages: the spatial information is considered and the computation burden is reduced.

Concretely, for pixel i and j, the Euclidean distance of polarimetric features is computed by $d(x_i, x_j) = \|x_i - x_j\|_2$. k nearest samples of pixel i are sought in a $2[\sqrt{k}] \times 2[\sqrt{k}]$ region centered on pixel i, where $[\bullet]$ denotes rounding a number. Then pixel i is represented as a second-order tensor $X_i \in R^{(k+1)\times 36}$ as shown in Fig. 1.

2.3. Solving for two projection matrices

For n samples $X_1, X_2, \cdots, X_n$, we aim to search for two project matrices $U_1 \in R^{d_1\times(k+1)}, U_2 \in R^{d_2\times 36}$, where d_1 and d_2 are the reduced dimensionality for the two orders. Then the low-dimensional representation is computed as follows:

$$Y_i = X_i \times_1 U_1 \times_2 U_2 \tag{1}$$

Algorithm 1: TPCA

Input: The training samples $\{X_1, \cdots, X_n\} \in R^{D_1\times\cdots\times D_M}$ and the reduced dimensionality $d_1, \cdots, d_M$

Initialize $U_1^0 = I_{D_1}, \cdots, U_M^0 = I_{D_M}$
for $t = 1, \cdots, T_{max}$ **do**
  for $m = 1, \cdots, M$ **do**
    $Z_i = X_i \times_1 \cdots \times_{m-1} U_{m-1}^t \times_{m+1} U_{m+1}^{t-1} \cdots \times_M U_M^{t-1}$, $i = 1, 2, \cdots, n$
    $Z_i \Rightarrow_m Z_i^{(m)}$, where $Z^{(m)}$ is the mode-m unfolding of Z
    Select the d_m eigenvectors corresponding to the largest d_m eigenvalues of $C_m^t = \sum_i \left(Z_i^{(m)} - \overline{Z}^{(m)}\right)\left(Z_i^{(m)} - \overline{Z}^{(m)}\right)^T$ to form the matrix $V \in R^{D_m\times d_m}$
    $U_m^t = V^T$
  end for
  If $t > 2$ and $\sum_{m=1}^M \|U_m^t - U_m^{t-1}\| < \varepsilon$, break
end for

Output: $U_m = U_m^t,\ m = 1, \cdots, M$.

where $Y_i \in R^{d_1\times d_2}$, $\times_1$ and $\times_2$ are the mode-1 and mode-2 product of a tensor and a matrix. Some definitions of tensors are presented in [6] in detail.

Here we employ TPCA for feature extraction. TPCA aims to maximize the total tensor scatter as follows:

$$\{U_1, U_2\} = \arg\max_{U_1,U_2} \sum_{i=1}^{n} \|(X_i - \overline{X}) \times_1 U_1 \times_2 U_2\|^2 \tag{2}$$

where $\overline{X} = \frac{1}{n}\sum_{i=1}^n X_i$ is the mean of n samples, $\|\bullet\|$ is the norm of a tensor. Problem (2) can be solved through an iterative process. Algorithm 1 displays the TPCA algorithm for general cases, i.e. $X \in R^{D_1\times\cdots\times D_M}$. Specific to $M = 2$, at each iteration, when $m = 1$, i.e., fix U_2 and solve for U_1, $Z_i = X_i \times_2 U_2$ and $Z_i^{(1)} = Z_i$. Because $\|(Z_i - \overline{Z}) \times_1 U_1\|^2 = \|U_1(Z_i^{(1)} - \overline{Z}^{(1)})\|_F^2 = tr(U_1(Z_i - \overline{Z})(Z_i - \overline{Z})^T U_1^T)$, problem (2) becomes:

$$U_1 = \arg\max_{U_1} tr\left(U_1\left(\sum_{i=1}^{n}(Z_i - \overline{Z})(Z_i - \overline{Z})^T\right)U_1^T\right) \tag{3}$$

Problem (3) can be solved by the eigenvalue decomposition of $\sum_{i=1}^n (Z_i - \overline{Z})(Z_i - \overline{Z})^T$. The d_1 eigenvectors corresponding to the largest k eigenvalues form the matrix V, then $U_1 = V^T$.

When $m = 2$, i.e., fix U_1 and solve for U_2, $Z_i = X_i \times_1 U_1$ and $Z_i^{(2)} = Z_i^T$. Then we do the eigenvalue decomposition of $\sum_{i=1}^n (Z_i - \overline{Z})^T (Z_i - \overline{Z})$ to obtain U_2.

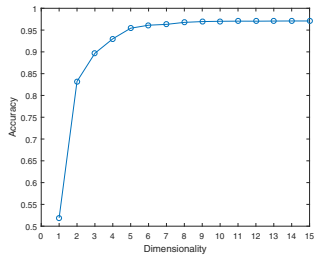

Fig. 2. Classification accuracy versus dimensionality on the San Francisco Bay data set.

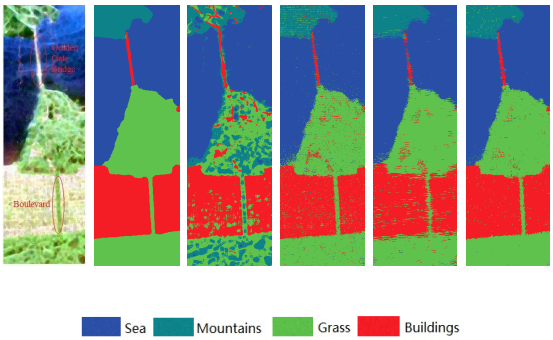

Fig. 3. Classification maps of the four methods on the San Francisco Bay data set: (a) the denoised image, (b) the ground truth, (c) SWC, (d) PCA, (e) 3DPCA, (f) the proposed method.

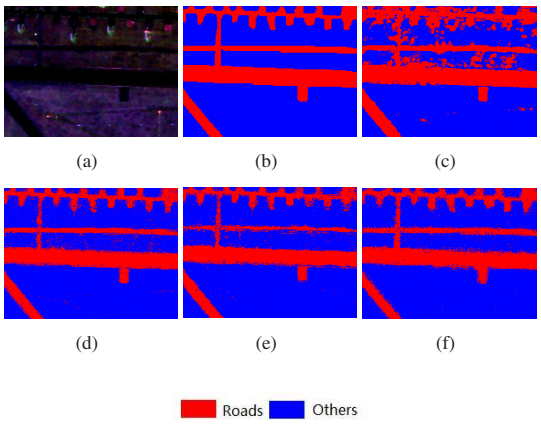

Fig. 4. Classification maps of the four methods on the Oberpfaffenhofen data set: (a) the denoised image, (b) the ground truth, (c) SWC, (d) PCA, (e) 3DPCA, (f) the proposed method.

3. EXPERIMENTS

Experiments are conducted on two PolSAR data sets which are acquired from the San Francisco Bay in the USA by NASA/JPL's AIRSAR and the Oberpfaffenhofen area in Germany by the German Aerospace Center's E-SAR, respectively.

For the first data set, we select a 600×200 subset which contains the Golden Gate Bridge and the boulevard as seen in Fig.3(a). We consider four classes: sea, mountains, grass and buildings as shown in Fig.3(b) [8]. The 7×7 refined Lee filter is used to filter the PolSAR image. In our experiments, 30% samples from each class are randomly selected for training and the rest for testing. The mean accuracy of 10 experiments is used as the classification numerical results. About some parameters of the proposed method, such as the number of nearest samples k, the reduced dimensionality d_1 and d_2, the maximum number of iterations T_{max} and the error ε, we select $k = 25$ empirically for a good performance. It is obvious that the intrinsic dimensionality of the first order is 1, then we set $d_1 = 1$. For d_2, Fig.2 shows the classification accuracies versus dimensionality ranging from 1 to 15. We can see that when d_2 is larger than 8, the accuracy stays almost unchange. Therefore, d_2 is set to be 8. In addition, $T_{max} = 10$ and $\varepsilon = 10^{-6}$. According to experiments, we can see that the algorithm stops after 3 iterations.

The proposed method is compared with supervised Wishart classifier (SWC), PCA, 3DPCA. The reduced dimensionality for PCA is 8. For 3DPCA, the $11 \times 11 \times 36$ third-order tensor is used for a good performance and the dimensionality for three orders are 1, 1 and 8. T_{max} and ε are set the same as the proposed method. To show how different feature extraction methods influence the classification performance more clearly, a very simple classifier, nearest neighbour (NN) classifier, is used for the final classification. The numerical and visual classification results are shown in Tab.1 and Fig.3, respectively.

From the results, we can see that pixel-based SWC and PCA do not have high classification accuracy and the visual classification map is also not close to the ground truth as shown in Figs.3(c-d). 3DPCA is a patch-based method, which makes use of spatial information. Therefore, 3DPCA has a better classification performance generally. However, the Golden Gate Bridge and the boulevard can not be maintained well as shown in Figs.3(e) because the direct usage of patch does not take the spatial heterogeneity into account. The proposed method firstly considers the spatial heterogeneity to construct the second-order tensors. Meanwhile both the spatial information and polarimetric information are exploited for feature extraction. Therefore, the proposed method has a higher classification accuracy and a better visual classification result compared with other methods.

The second data set consists of a great number of roads [9] and we select a 300×400 subarea which only contains

Table 1. Classification accuracies comparison of four methods on the San Francisco Bay data set

Method	Sea	Mountains	Grass	Buildings	Total accuracy
SWC	0.9583	0.6094	0.5778	0.8720	0.7824
PCA	0.9703	0.7787	0.9007	0.8992	0.9165
3DPCA	0.9730	0.9133	0.9212	0.8945	0.9324
The proposed method	0.9843	0.9400	0.9600	0.9625	0.9677

Table 2. Classification accuracies comparison of four methods on the Oberpfaffenhofen data set

Method	Roads	Others	Total accuracy
SWC	0.9277	0.8499	0.8713
PCA	0.8585	0.9496	0.9228
3DPCA	0.8114	0.9591	0.9158
The proposed method	0.8828	0.9550	0.9338

roads and others as shown in Fig.4(b) to further validate the proposed method can preserve the spatial heterogeneity. The experimental setting and parameters are the same as those of the first data set. The numerical and visual classification results are shown in Tab.2 and Fig.4. We can see that for this extreme case 3DPCA performs even worse than PCA and the roads are broken. The proposed method still performs better than other methods.

4. CONCLUSION

This paper proposed a novel tensor-based extraction method for PolSAR image classification. To take the spatial heterogeneity into account, we firstly seek k nearest samples based on the polarimetric feature similarity in a spatial local region. Then each pixel is represented as a second-order tensor. Finally, TPCA is used to extract low-dimensional features. Experimental results demonstrate the proposed method can improve the performance of PolSAR image classification .

5. ACKNOWLEDGEMENT

This work was partly supported by the Beijing Natural Science Foundation under Grant 4174107, and partly supported by the National Natural Science Foundation of China under Grant 61802408, Grant U1435220, Grant 91648205 and Grant 61602483.

6. REFERENCES

[1] H. Liu, Z. Wang, F. Shang, Y. Shuyuan, S. Gou, and L. Jiao, "Semi-supervised tensorial locally linear embedding for feature extraction using PolSAR data," *IEEE Journal of Selected Topics in Signal Processing*, pp. 1–1, 2018.

[2] S. Uhlmann and S. Kiranyaz, "Integrating color features in polarimetric SAR image classification," *IEEE Transactions on Geoscience and Remote Sensing*, vol. 52, no. 4, pp. 2197–2216, April 2014.

[3] S. T. Tu, J. Y. Chen, W. Yang, and H. Sun, "Laplacian eigenmaps-based polarimetric dimensionality reduction for SAR image classification," *IEEE Transactions on Geoscience and Remote Sensing*, vol. 50, no. 1, pp. 170–179, Jan 2012.

[4] L. Shi, L. Zhang, J. Yang, L. Zhang, and P. Li, "Supervised graph embedding for polarimetric SAR image classification," *IEEE Geoscience and Remote Sensing Letters*, vol. 10, no. 2, pp. 216–220, March 2013.

[5] M. Tao, F. Zhou, J. Su, and J. Xie, "Feature extraction for PolSAR image classification using multilinear subspace learning," in *2017 IEEE International Geoscience and Remote Sensing Symposium (IGARSS)*, July 2017, pp. 1796–1799.

[6] X. Huang, H. Qiao, B. Zhang, and X. Nie, "Supervised polarimetric SAR image classification using tensor local discriminant embedding," *IEEE Transactions on Image Processing*, vol. 27, no. 6, pp. 2966–2979, June 2018.

[7] L. Zhang, C. Han, and Y. Cheng, "Improved SLIC superpixel generation algorithm and its application in polarimetric SAR images classification," in *2017 IEEE International Geoscience and Remote Sensing Symposium (IGARSS)*, July 2017, pp. 4578–4581.

[8] C. He, J. Deng, L. Xu, S. Li, M. Duan, and M. Liao, "A novel over-segmentation method for polarimetric SAR images classification," in *2012 IEEE International Geoscience and Remote Sensing Symposium*, July 2012, pp. 4299–4302.

[9] C. He, S. Li, Z. Liao, and M. Liao, "Texture classification of PolSAR data based on sparse coding of wavelet polarization textons," *IEEE Transactions on Geoscience and Remote Sensing*, vol. 51, no. 8, pp. 4576–4590, Aug 2013.